Comptes Rendus

Chimie

W. Ryan Osterloh, Yuanyuan Fang, Nicolas Desbois, Mario L. Naitana, Stéphane Brandès, Sandrine Pacquelet, Claude P. Gros and Karl M. Kadish

Here's looking at the reduction of noninnocent copper corroles *via* anion induced electron transfer

Part of Special Issue: MAPYRO: the French Fellowship of the Pyrrolic Macrocyclic Ring

Guest editors: Bernard Boitrel (Institut des Sciences Chimiques de Rennes, CNRS-Université de Rennes 1, France) and Jean Weiss (Institut de Chimie de Strasbourg, CNRS-Université de Strasbourg, France)

MAPYRO: the French Fellowship of the Pyrrolic Macrocyclic Ring / *MAPYRO: la communauté française des macrocycles pyrroliques*

Here's looking at the reduction of noninnocent copper corroles *via* anion induced electron transfer

W. Ryan Osterloh [a], **Yuanyuan Fang** [a], **Nicolas Desbois** [b], **Mario L. Naitana** [b], **Stéphane Brandès** [b], **Sandrine Pacquelet** [b], **Claude P. Gros** [*, b] and **Karl M. Kadish** [*, a]

[a] Department of Chemistry, University of Houston, Houston, Texas 77204-5003, USA

[b] Université Bourgogne Franche-Comté, ICMUB (UMR CNRS 6302), 9 Avenue Alain Savary, BP 47870, 21078 Dijon, Cedex, France

E-mails: osterloh91@gmail.com (W. Ryan Osterloh), fangyy1019@yahoo.com (Y. Fang), Nicolas.Desbois@u-bourgogne.fr (N. Desbois), mario.naitana83@gmail.com (M. L. Naitana), Stephane.Brandes@u-bourgogne.fr (S. Brandès), Sandrine.Pacquelet@u-bourgogne.fr (S. Pacquelet), claude.gros@u-bourgogne.fr (C. P. Gros), kadish@central.uh.edu (K. M. Kadish)

Abstract. The synthesis, electrochemical and spectroscopic characterization of five copper triarylcorroles bearing one, two or three *meso*-nitroaryl substituents is reported. Redox potentials and spectroscopic properties of the neutral Cu(II) corrole cation radicals and singly reduced form of the complexes are reported in CH_2Cl_2 and the ability of the initial noninnocent derivatives to be chemically reduced *via* anion induced electron transfer (AIET) is explored using cyanide (CN^-) or fluoride (F^-) anions in the form of tetra-*n*-butylammonium salts. UV–visible spectra of the singly reduced corroles and the species generated after addition of CN^- or F^- to solutions of the neutral compounds are identical, thus confirming the AIET event in these systems. This result, when combined with the facile electrochemical reduction, provides strong indirect evidence for the presence of noninnocence in these systems.

Keywords. Corroles, Anion induced electron transfer, Noninnocent, Electrochemistry, Spectroelectrochemistry.

Available online 30th July 2021

1. Introduction

Numerous free-base and transition metal triarylcorroles bearing different *meso*- and β-substituents have been synthesized [1,2] and electrochemically examined [3], with particular emphasis being placed on elucidating the electronic configuration of those metal complexes which are known to act as air-stable radicals [4–8]. In 2010, Pierloot *et al.* [9] presented *ab initio* evidence for a noninnocent corrole ligand in the case of copper corroles, and since that time there have been many reports characterizing neutral copper corroles as having a reduced divalent central metal ion (Cu^{II}) and an oxidized macrocyclic ligand in its cation radical form ($Cor^{•2-}$) [5–7,10–14]. Evidence for this assignment has involved a wide variety of approaches, including structural analysis, spectroscopic measurements and electrochemical criteria to assess the noninnocent behavior of

* Corresponding authors.

the corrole in question and a concise summary of what has been published in this area was recently reviewed by Ganguly and Ghosh [15]. In our own work we have suggested an electrochemical litmus test for evaluating the innocence or noninnocence of transition-metal corroles [3,5,10,11,13,16–19], and suggested that the presence of a facile reduction at potentials more positive than −0.20 V *versus* SCE (Saturated Calomel Electrode) could be used as one electrochemical diagnostic criterion to establish ligand noninnocence in these systems.

Our recent studies on the electrochemistry of tetrapyrrole macrocycles has focused in part on cobalt corroles [16–19], some of which possessed redox-active *meso*-nitrophenyl groups [16,17] where ligand noninnocence or innocence was shown to be governed by the number and type of axial ligands bound to the formal cobalt(III) central metal ion. In one of these studies [19], we reported the effect of anions on the spectroscopic and electrochemical properties of noninnocent cobalt corroles and noted that the addition of cyanide anions (CN$^-$) to solution led to the stepwise formation of a five- and six-coordinate cobalt(III) complex with an innocent corrole macrocyclic ligand, while the addition of other anions, such as fluoride (F$^-$), led to a chemical reduction of the noninnocent corrole ligand giving an anionic [Cor^{3-}Co^{II}]$^-$ product. The reaction with F$^-$ was rationalized by the known ability of strong Lewis basic anions to reduce or form a solvent caged radical pair with certain π-acids (i.e. ligands with a low lying LUMO or SOMO-1) *via* anion induced electron transfer (AIET) [20–22].

There remains little doubt surrounding the assignment of ligand noninnocence in the case of copper corroles which are isolated as four-coordinate species and do not undergo axial ligation in solution and these [Cor$^{\bullet 2-}$Cu^{II}] systems therefore serve as ideal metallocorroles to explore the ability of AIET to occur in aprotic media. This is examined in the current study which reports synthesis and characterization of the five copper corroles (**1–5**) in Scheme 1, with one aim of this study being to elucidate the prevailing electrochemical and spectroscopic behavior of copper nitroaryl corroles in CH$_2$Cl$_2$ and the other to explore the possible reduction of these open-shell complexes by cyanide or fluoride anions added to solution in the form of tetra-*n*-butylammonium salts, TBACN or TBAF.

2. Experimental section

2.1. *Material and instrumentation*

All chemicals and solvents were of the highest electrochemical grade available and were used without further purification. NMR solvents were purchased from Eurisotope. DriSolve anhydrous dichloromethane (CH$_2$Cl$_2$, ≥99.8%) was purchased from Sigma Chemical Co. Tetra-*n*-butyl-ammonium perchlorate (TBAP, ≥99.0%), 95.0% tetra-*n*-butyl-ammonium cyanide (TBACN) and 98% tetra-*n*-butyl-ammonium fluoride hydrate (TBAF) were purchased from Sigma Chemical Co. and stored in a desiccator until used. Copper corrole **0** (see Scheme 1) was synthesized and characterized according to literature procedures [23].

^{1}H NMR spectra were recorded on a Bruker Avance NEO 500 spectrometer operating at 500 MHz and available at the PACSMUB-WPCM technological platform, which relies on the "Institut de Chimie Moléculaire de l'Université de Bourgogne" and SATT SAYENS "TM", a Burgundy University private subsidiary. All NMR shift values are expressed in ppm. ^{1}H NMR spectra were calibrated using the residual peak of chloroform at 7.26 ppm and ^{19}F NMR spectra were calibrated with an internal reference (CFCl$_3$).

UV–visible spectra of the synthesized compounds were recorded on a Varian Cary 50 or Hewlett-Packard model 8453 diode array spectrophotometer. Quartz cells with optical path lengths of 10 mm were used. ESI mass spectra were recorded on a LTQ Orbitrap XL (THERMO) instrument for HR-MS spectra and on an AmaZon SL (Bruker) instrument for the LRMS spectra or on a Bruker Microflex LRF MALDI Tandem TOF mass spectrometer using dithranol as the matrix.

Thin-layer UV–vis spectroelectrochemical measurements were made using a commercially available thin-layer cell from Pine Instruments Inc. which had a platinum honeycomb working electrode consisting of 19 Pt-coated channels with each channel being 0.50 mm in diameter and a center-to-center distance of 0.75 mm. Potentials were applied and monitored with an EG&G PAR Model 173 potentiostat/galvanostat. High-purity argon from Matheson Trigas was used to deoxygenate the solution and a stream of inert gas was kept over the solution during each spectroelectrochemical experiment.
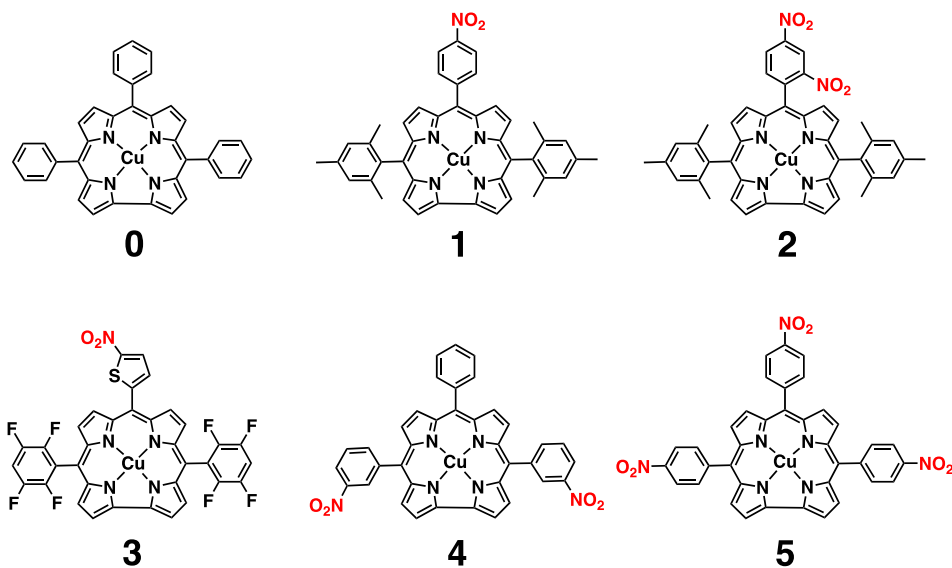
Scheme 1. Structures and numbering of the investigated copper triarylcorroles **1–5** and the reference compound **0**.

Electrochemical measurements were performed at 298 K using an EG&G Princeton Applied Research (PAR) Model 173 potentiostat/galvanostat, paired with a EG&G PAR Model 175 universal programmer and a Houston Instruments Omnigraphic 2000 XY Plotter. The three electrode system used for cyclic voltammetric measurements consisted of a glassy carbon working electrode, a platinum counter electrode and a saturated calomel reference electrode (SCE) which was separated from the bulk of the solution by a fritted glass bridge of low porosity. The bridge was purchased from Gamry Instruments and contained the solvent/supporting electrolyte mixture.

2.2. Synthesis of 5,15-dimesityl-10-(2,4-dinitrophenyl)corrole, $(Mes)_2(2,4\text{-}(NO_2)_2Ph)CorH_3$

In a round bottom flask, 5-mesityldipyrromethane (396.5 mg, 1.5 mmol) and 2,4-dinitrobenzaldehyde (147 mg, 0.75 mmol) were dissolved in 150 mL of CH_3OH. Afterwards a solution of 3.8 mL of HCl_{aq} (36%w) in 75 mL of water was added and the crude material was stirred at room temperature for 2 h. The mixture was extracted with 80 mL of $CHCl_3$ after which the organic phase was washed twice with 80 mL of water, dried on sodium sulfate, filtered

and then diluted with 250 mL of $CHCl_3$. *p*-Chloranil (369 mg, 1.5 mmol) was added and the mixture was stirred overnight at room temperature. The reaction mixture was evaporated to dryness and chromatographed on silica gel using a $CHCl_3$-heptane (2:1, v:v) eluent. Yield 160.2 mg (0.23 mmol, 31%). UV–vis (CH_2Cl_2) λ_{max} [nm, $\varepsilon \times 10^3$ ($M^{-1} \cdot cm^{-1}$)]: 406 (106.2), 421 (86.9), 569 (20.5), 599 (14.8). ^1H NMR (500 MHz, $CDCl_3$), δ (ppm): 9.17 (d, ^4J = 2.5 Hz, 1H, H_{Ph}), 8.88 (d, ^3J = 4.5 Hz, 2H, H_β), 8.72 (d, ^3J = 8.0 Hz, 1H, H_{Ph}), 8.50 (d, ^3J = 5.0 Hz, 2H, H_β), 8.44 (d, ^3J = 8.0 Hz, 1H, H_{Ph}), 8.32 (d, ^3J = 4.5 Hz, 2H, H_β), 8.21 (d, ^3J = 4.5 Hz, 2H, H_β), 7.27–7.25 (s, 4H, mesityl, overlapped with $CHCl_3$ deuterated solvent residual signal), 2.59 (s, 6H, CH_3), 1.94 (s, 6H, CH_3), 1.89 (s, 6H, CH_3). LRMS (MALDI/TOF) $[M+H]^+$: 701.13 (exp.), 701.29 (calcd). HRMS (ESI) $[M+H]^+$: 701.2882 (exp.), 701.2871 (calcd). See Figures S1 and S2 for ^1H NMR and ESI-MS data.

2.3. General synthetic procedures for copper corroles

2.3.1. Protocol A

Corrole (0.091 mmol) and $Cu(acac)_2$ (191.0 mg, 0.73 mmol, 8.0 eq) were dissolved in dichloromethane (9 mL) and triethylamine (0.3 mmol). The mixture was stirred at room temperature for 20 min

and then vacuum dried. The residue was purified by column chromatography as described below.

2.3.2. *Protocol B*

Corrole (0.041 mmol) and CuOAc$_2$·H$_2$O (66.4 mg, 0.33 mmol, 8.0 eq) were dissolved in dichloromethane (5 mL) and methanol (20 mL). The mixture was stirred at room temperature until the color changed to yellow-brown, after which the temperature was increased to 75 °C for 5 h. After evaporating to dryness, the residue was purified by column chromatography as described below.

2.4. (Mes)$_2$(4-NO$_2$Ph)CorCu (**1**)

This compound was synthesized following *Protocol B* starting from 30.0 mg of free base corrole [24]. Purification was carried out on a silica gel column using a CH$_2$Cl$_2$/heptane (1:1, v:v) eluent. The synthesis of corrole **1** followed a modified synthetic procedure reported in the literature [25]. Yield: 31.2 mg (0.044 mmol, 95%). UV–vis (CH$_2$Cl$_2$) λ_{max} [nm, $\varepsilon \times 10^3$ (M^{-1}·cm^{-1})]: 396 (67.9), 537 (7.9), 597 (4.7). ^{1}H NMR (500 MHz, CDCl$_3$), δ (ppm): 8.36 (d, ^3J = 8.0 Hz, 2H, H$_{Ph}$), 7.99 (m, 2H, H$_\beta$), 7.77 (d, ^3J = 8.0 Hz, 2H, H$_{Ph}$), 7.36 (d, ^3J = 4.0 Hz, 2H, H$_\beta$), 7.21 (m, 2H, H$_\beta$), 7.03 (m, 6H, H$_\beta$, H$_{Mes}$), 2.40 (s, 6H), 2.06 (s, 12H). LRMS (MALDI/TOF) [M]$^{+\bullet}$: 715.17 (exp.), 715.20 (calcd). See Figures S3 and S4 for ^{1}H NMR and ESI-MS data.

2.5. (Mes)$_2$(2,4-(NO$_2$)$_2$Ph)CorCu (**2**)

This compound was synthesized following *Protocol B* starting from 30.5 mg of free base corrole (**Mes**)$_2$(**2,4**-(**NO$_2$**)$_2$**Ph**)**CorH$_3$**. Purification was carried out on a silica gel column using a CH$_2$Cl$_2$/ heptane (1:1, v:v) eluent. Yield: 31.0 mg (0.0041 mmol, 94%). UV–vis (CH$_2$Cl$_2$) λ_{max} [nm, $\varepsilon \times 10^3$ (M^{-1}·cm^{-1})]: 397 (91.8), 601 (5.6). ^{1}H NMR (500 MHz, CDCl$_3$), δ (ppm): 8.99 (d, ^4J = 2.0 Hz, 1H, H$_{Ph}$), 8.58 (d, ^3J = 8.0 Hz, 1H, H$_{Ph}$), 8.05 (m, 2H, H$_\beta$), 7.86 (d, ^3J = 8.0 Hz, 1H, H$_{Ph}$), 7.36 (d, ^3J = 4.0 Hz, 2H, H$_\beta$) 7.23 (m, 2H, H$_\beta$), 7.04 (s, 2H, H$_{Mes}$), 7.03 (s, 2H, H$_{Mes}$), 6.82 (d, ^3J = 4.5 Hz, 2H, H$_\beta$), 2.40 (s, 6H, CH$_3$), 2.07 (s, 6H, CH$_3$), 2.05 (s, 6H, CH$_3$). LRMS (MALDI/TOF) [M]$^{+\bullet}$: 760.20 (exp.), 760.19 (calcd). HRMS (ESI) [M]$^{+\bullet}$: 760.1887 (exp.), 760.1854 (calcd), [M+Na]$^+$: 783.1753 (exp.), 783.1752 (calcd). See Figures S5 and S6 for ^{1}H NMR and ESI-MS data.

2.6. (2,3,4,5-F$_4$Ph)$_2$(2-NO$_2$thiophene)CorCu (**3**)

This compound was synthesized following *Protocol B* starting from 30.2 mg of free base corrole [26–28]. Purification was carried out on a silica gel column using a CH$_2$Cl$_2$/heptane (1:1, v:v) eluent. Yield: 30.3 mg (0.0039 mmol, 93%). UV–vis (CH$_2$Cl$_2$) λ_{max} [nm, $\varepsilon \times 10^3$ (M^{-1}·cm^{-1})]: 405 (73.2). ^{1}H NMR (500 MHz, CDCl$_3$), δ (ppm): 7.97 (d, ^3J = 4.0 Hz, 1H, H$_{thio}$), 7.93 (d, ^3J = 4.0 Hz, 2H, H$_\beta$), 7.43 (d, ^3J = 4.5 Hz, 2H, H$_\beta$), 7.40 (d, ^3J = 4.5 Hz, 2H, H$_\beta$) 7.36 (d, ^3J = 4.0 Hz, 1H, H$_{thio}$), 7.31–7.26 (m, 4H, H$_{Ph}$, H$_\beta$). ^{19}F NMR (470 MHz, CDCl$_3$), δ (ppm): −137.55 to −137.57 (m, 8F). LRMS (MALDI/TOF) [M]$^{+\bullet}$: 780.98 (exp.), 780.99 (calcd). HRMS (ESI) [M]$^{+\bullet}$: 780.9899 (exp.), 780.9875 (calcd). See Figures S7 and S8 for ^{1}H NMR, ^{19}F NMR and ESI-MS data.

2.7. (3-NO$_2$Ph)$_2$(Ph)CorCu (**4**)

This compound was synthesized following *Protocol B* starting from 30.0 mg of free base corrole [29]. Purification was carried out on a silica gel column using a CH$_2$Cl$_2$/heptane (2:1, v:v) eluent. Synthesis of corrole **4** has already been reported in the literature [29]. Yield: 17.3 mg (0.026 mmol, 52%). UV–vis (CH$_2$Cl$_2$) λ_{max} [nm, $\varepsilon \times 10^3$ (M^{-1}·cm^{-1})]: 407 (80.6), 541 (6.3), 625 (4.3). ^{1}H NMR (500 MHz, CDCl$_3$), δ (ppm): 8.59 (m, 2H, H$_{Ph}$), 8.44 (d, ^3J = 8.0 Hz, 2H, H$_{Ph}$), 8.05 (d, ^3J = 8.0 Hz, 2H, H$_{Ph}$), 7.89 (m, 2H, H$_\beta$), 7.69 (t, ^3J = 8.0 Hz, 2H, H$_{Ph}$), 7.60 (m, 3H, H$_{Ph}$), 7.54 (d, ^3J = 5.0 Hz, 2H, H$_\beta$), 7.47 (m, 2H, H$_{Ph}$), 7.27 (d, ^3J = 4.5 Hz, 2H, H$_\beta$), 7.26 (m, 2H, H$_\beta$). LRMS (MALDI/TOF) [M]$^{+\bullet}$: 676.06 (exp.), 676.09 (calcd). See Figures S9 and S10 for ^{1}H NMR and ESI-MS data.

2.8. (4-NO$_2$Ph)$_3$CorCu (**5**)

This compound was synthesized following *Protocol A* starting from 60.0 mg of free base corrole [30]. The purification process consisted of a silica gel column using neat CH$_2$Cl$_2$ as the eluent. Synthesis of corrole **5** has already been reported in the literature [31]. Yield: 30.0 mg (0.042 mmol, 46%). UV–vis (CH$_2$Cl$_2$) λ_{max} [nm, $\varepsilon \times 10^3$ (M^{-1}·cm^{-1})]: 420 (37.5), 540 (5.0), 627 (3.5). ^{1}H NMR (500 MHz, CDCl$_3$), δ (ppm): 8.37 (m, 6H, H$_{Ph}$), 8.00 (m, 2H, H$_\beta$), 7.92 (d, ^3J = 8.5 Hz, 4H, H$_{Ph}$), 7.83 (d, ^3J = 8.5 Hz, 2H, H$_{Ph}$), 7.59 (d, ^3J = 4.5 Hz, 2H, H$_\beta$), 7.31 (m, 2H, H$_\beta$), 7.19 (d, ^3J = 4.5 Hz,

Table 1. Half-wave potentials (V *versus* SCE) of copper triarylcorroles **0–5** in CH_2Cl_2 containing 0.1 M TBAP

Cpd	$E_{1/2}$ (V *versus* SCE)				i_{pc}^{R2}/i_{pc}^{R1a}	Ref.
	2nd Ox	1st Ox	1st Red	2nd Red (#e)		
0	1.46^c	0.78	−0.19	−1.94 (1)^b	—	[10]
1	1.40^c	0.80	−0.16	−1.16 (1)	0.95	t.w
2	1.43^c	0.83	−0.09	−0.92 (1)	1.00	t.w
3	1.57^c	1.08	0.19	−1.00 (1)	1.00	t.w
4	1.46^c	0.88	−0.08	−1.13 (2)	1.95	t.w
5	1.44	0.95	0.02	−1.10 (3)	2.94	t.w

Structures of the compounds are given in Scheme 1.

^{a} i_{pc}^{R2}/i_{pc}^{R1} = ratio of cathodic peak current for 2nd Red (at the *meso*-nitroaryl group) over that of the first 1st Red (at the conjugated macrocycle).

^{b} Obtained in CH_2Cl_2/0.1 M TBAP at −60 °C.

^{c} Peak potential of irreversible process at scan rate of 0.1 V/s. t.w = this work.

2H, H_β). LRMS (MALDI/TOF) $[M]^{+\bullet}$: 721.06 (exp.), 721.08 (calcd). See Figures S11 and S12 for ^1H NMR and ESI-MS data.

3. Results and discussion

3.1. *Electrochemistry*

Each copper corrole was electrochemically examined in CH_2Cl_2 containing 0.1 M TBAP at room temperature. Examples of cyclic voltammograms for **1–5** are given in Figure 1 and half-wave potentials are summarized in Table 1 which also includes data for the parent copper triphenylcorrole (**0** in Scheme 1) under the same solution conditions [10].

As seen in Figure 1, the nitroaryl corroles **1–5** exhibit two reversible reductions and at least one reversible oxidation while the parent compound **0** exhibits only one reversible reduction and one reversible oxidation within the solvent potential window. Half-wave potentials for the first reduction of the corroles are located between 0.19 and −0.19 V *versus* SCE and are assigned to occur at the conjugated macrocycle as given in (1).

$$Cor^\bullet Cu^{II} + e^- \rightleftharpoons [CorCu^{II}]^-\qquad(1)$$

This assignment of electron transfer site is consistent with earlier assignments for numerous copper [5,11–13,32] and other noninnocent

metallocorroles [5,15–19,33,34] and fits with the Kadish electrochemical diagnostic criterion [18] that noninnocent macrocycles will undergo a facile reduction in nonaqueous media (*vide supra*). As seen in Figure 1 and Table 1, the most facile one-electron addition occurs for **3** ($E_{1/2}$ = 0.19 V), consistent with the electron withdrawing properties of both the meso-nitrothiophene group and the two *meso*-tetrafluorophenyl substituents while corrole **1** bearing two mesityl and one *para*-nitrophenyl *meso*-group exhibits the most difficult ligand centered reduction of the investigated nitroaryl corroles at $E_{1/2}$ = −0.16 V. All of the nitroarylcorroles are easier to reduce than the parent compound, **0** ($E_{1/2}$ = −0.19 V), an expected result due to the highly electron-withdrawing NO_2 substituent.

The second reduction of compounds **1–5** ranges from $E_{1/2}$ = −1.16 (for **1**) to −0.92 V (for **2**) and these values can be compared to −1.94 V for the second reduction of corrole **0** when the measurement was carried out at −60 C [10]. This large difference in potential for the second reduction of the five copper corroles bearing one or more nitroaryl substituents is consistent with a change in the site of electron transfer, from π-ring centered in the case of **0** to the electroactive *meso*-nitroaryl ring(s) in the case of compounds **1–5**. This assignment of electron transfer site in **1–5** is consistent with
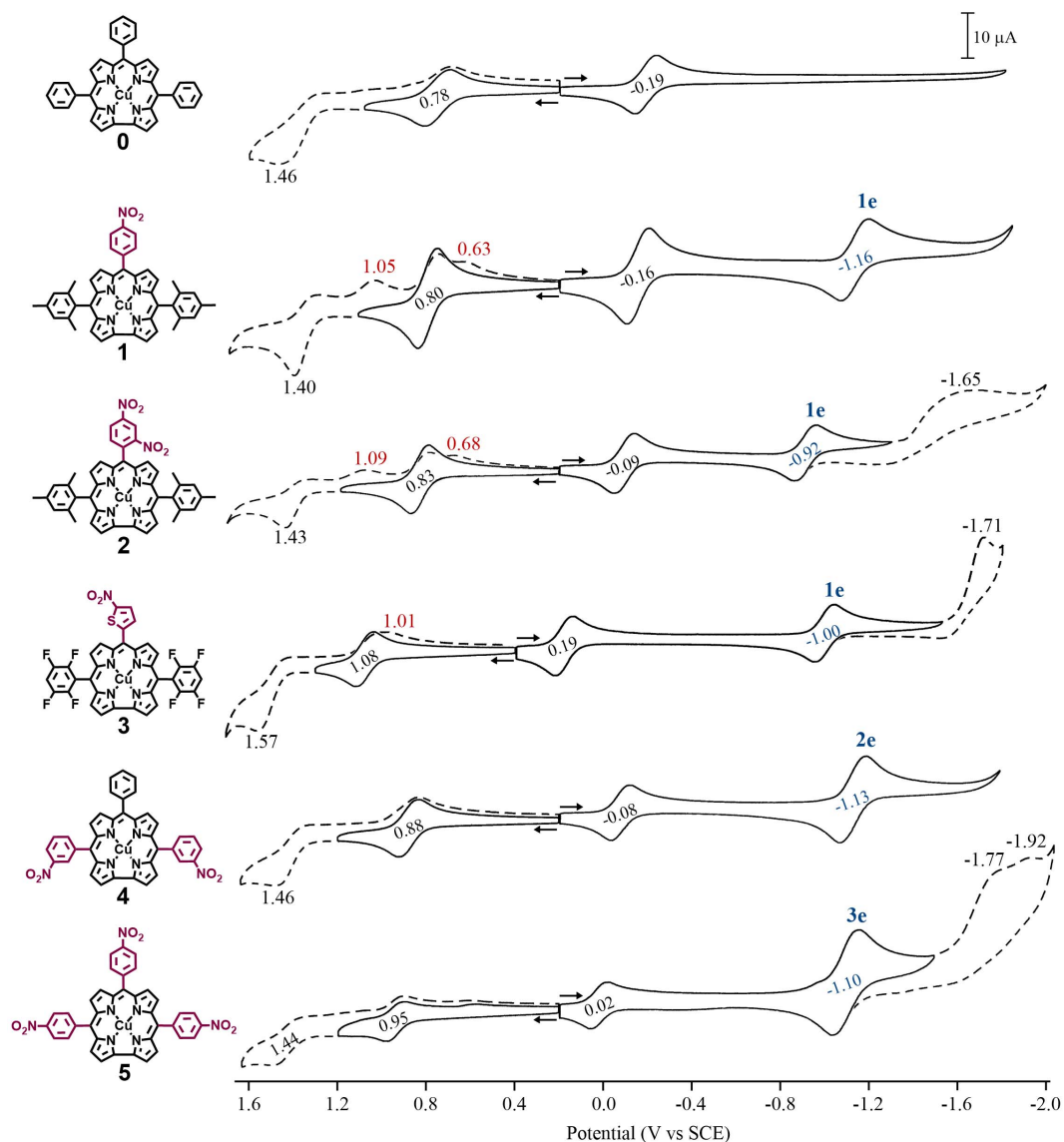
Figure 1. Cyclic voltammograms of copper corroles **1**–**5** in CH_2Cl_2 containing 0.1 M TBAP. Scan rate = 0.1 V/s. Potentials for the *meso*-nitroaryl reduction are shown in blue, the number of electrons transferred in the second reduction step is indicated above the half-wave potential and peak potentials for chemically generated products formed after oxidation are given in red.

the known electrochemistry of nitrobenzene [35], which is reduced in two steps, the first being reversible and located at $E_{1/2} = -1.08$ V *versus* SCE in CH_2Cl_2 [36]. The half-wave potential for the second reduction of **1** ($E_{1/2} = -1.16$ V) is close to that of free nitrobenzene while the second reversible reduction of corroles **2** ($E_{1/2} = -0.92$ V) and **3** ($E_{1/2} = -1.00$ V) are located at potentials close to reported

$E_{1/2}$ values in nonaqueous media for reduction of *m*-dinitrobenzene [37] and 2-nitrothiophene [38], respectively. Additional evidence for reduction of the nitroaryl groups is given by i_{pc}^{R2}/i_{pc}^{R1}, defined as the ratio of cathodic peak current (i_{pc}) for the second electroreduction over the i_{pc} value for the first reduction of the same compound. As seen in Table 1, this ratio is approximately 1.0 for compounds **1**–**3**,

2.0 for compound **4**, and 3.0 for compound **5**, values consistent with the number of nitroaryl substituents on the examined corrole and indicating a single one-electron reduction of this group in each case. Reductions occurring at the *meso*-NO$_2$Ph groups of iron [39,40], cobalt [16,17,19,40] and copper [31] corroles have previously been reported while similar *meso*-substituent-centered reductions have also been shown to occur for porphyrins bearing *meso*-nitrophenyl groups [40,41].

As mentioned above, nitrobenzene [35] and nitrothiophene [38] are both characterized by two reductions in nonaqueous media, the second of which is irreversible. The same is seen for the copper corroles **2**, **3** and **5** in CH$_2$Cl$_2$ (Figure 1) where the second and third reductions are assigned to occur at the meso-nitroaryl group. It is worth noting that the copper corrole **2** bearing both a *ortho*- and *para*-NO$_2$ substituent on one *meso*-phenyl ring of the compound displays only a single one-electron reduction at −0.97 V while *m*-dinitrobenzene displays two closely spaced reversible reductions [37,42] located at −0.90 and −1.25 V *versus* SCE when measured in acetonitrile containing tetra-*n*-propylammonoium perchlorate [37].

The first oxidation of corroles **1–5** is reversible and located at potentials ranging from 0.80 to 1.08 V *versus* SCE. On the basis of literature assignments for compound **0** and related copper corroles [5,10–12,43], this process in the current study is assigned as a ligand-centered oxidation, resulting in a cationic product with a divalent Cu^{II} metal center and a doubly oxidized corrole macrocycle according to (2).

$$Cor^\bullet Cu^{II} \rightleftharpoons [CorCu^{II}]^+ + e^- \qquad (2)$$
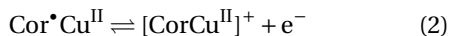
A plot of the first oxidation potential *versus* the first reduction potential for compounds **0–5** in CH$_2$Cl$_2$ containing 0.1 M TBAP is shown in Figure 2 and reveals a characteristic of these noninnocent corrole systems. The plot in the figure is linear with a high correlation coefficient of $R^2 = 0.985$, thus suggesting that the site of both electroreduction and electrooxidation remains the same throughout the series of compounds, and supporting the assignments given in (1) and (2). Inductive effects of *meso*-substituents on corroles, porphyrins and related macrocycles are known to govern redox potentials [3, 19,41,44–48] and it was expected that a linear plot would be obtained between the two redox potentials
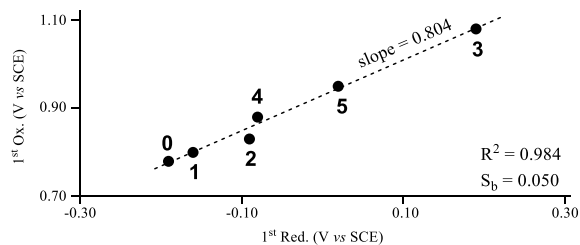

Figure 2. Plots of $E_{1/2}$ for first oxidation *versus* $E_{1/2}$ for first reduction of corroles **0–5** in CH$_2$Cl$_2$ containing 0.1 M TBAP.

in Figure 2 (assuming that the sites of electron transfer remain the same throughout the series); however the magnitude of the slope in the plot of Figure 2 provides insight into how the electron withdrawing substituents influence differently the oxidation and reduction potentials of noninnocent corroles in the currently investigated series of compounds. As seen in the figure, the slope of the linear regression analysis is 0.804 with a standard error (or deviation) of the slope (S_b) of 0.050. The obtained slope of less than 1.0 indicates that reduction of the noninnocent copper triarylcorroles (or the LUMO/SOMO-1) is more affected by electron withdrawing substituents on the *meso*-aryl groups than is the oxidation (or HOMO energies) by a factor of ~1.25.

Each investigated corrole also undergoes a second oxidation which is irreversible for **1–4** and located at an anodic peak potential (E_{pa}) between 1.40 and 1.57 V (see Figure 1). A chemical reaction follows this electron transfer and leads to a new electrooxidation product which is reduced at potentials between $E_{pc} = 1.01$ and 1.05 V for **1–3** on the reverse scan. Interestingly, corrole **5** displays a reversible second oxidation at $E_{1/2} = 1.44$ V indicating the absence of a coupled chemical reaction on the cyclic voltammetry timescale, but plots of E_{pc} values for this process in compounds **1–5** *versus* $E_{1/2}$ for the first reduction or first oxidation are linear, suggesting that the site of the second electron abstraction does not change in the series of investigated corroles.

3.2. *Electrochemical or chemical reduction via anion induced electron transfer (AIET)*

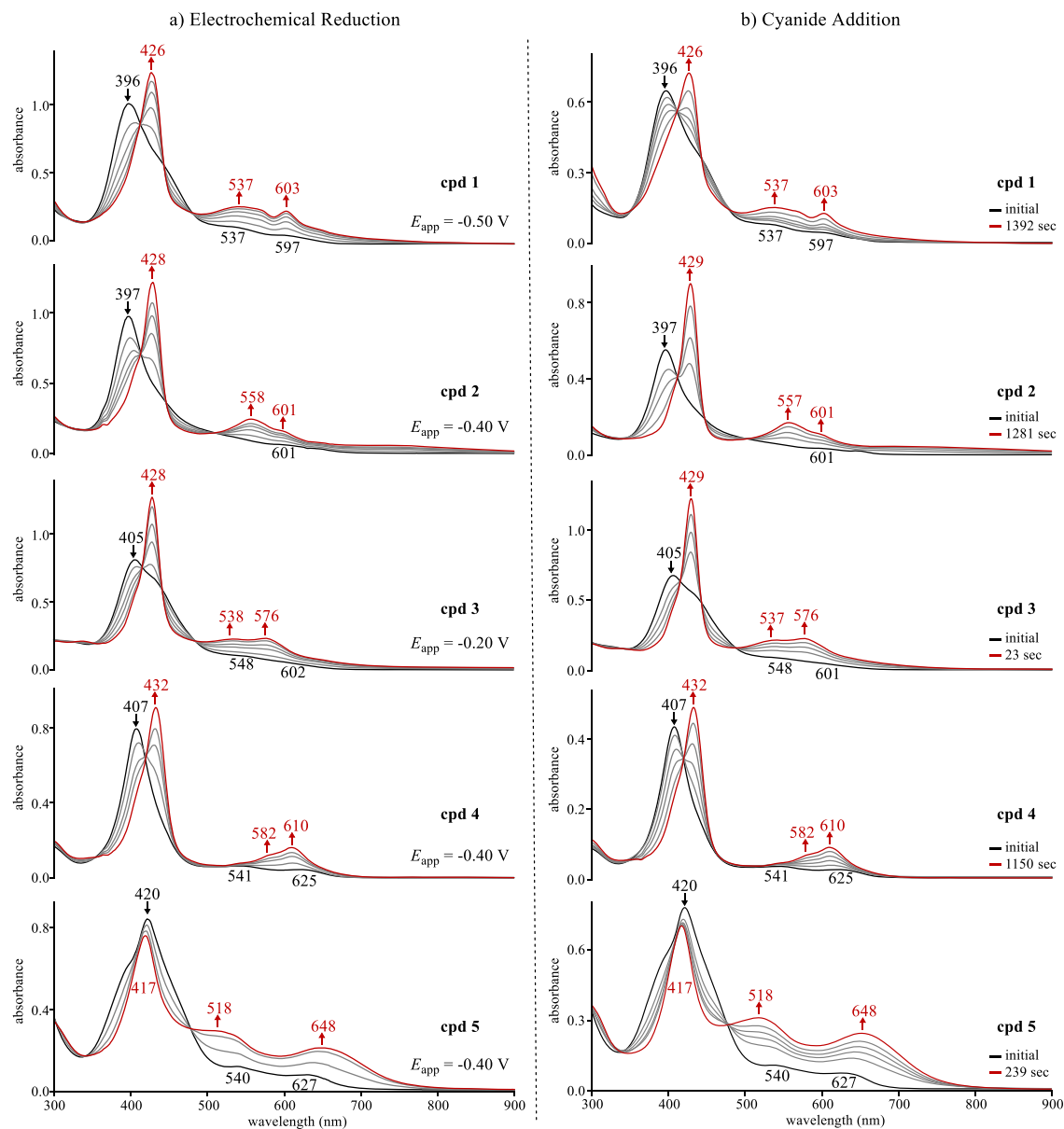To characterize the one-electron reduction product(s) of **1–5**, thin-layer UV–vis spectroelectrochem-

Figure 3. UV–vis spectral changes for compounds **1–5** (a) during an applied reducing potential (~10^{-4} M) in CH_2Cl_2 containing 0.1 M TBAP and (b) upon addition of TBACN (0.02 M) to ~10^{-5} M corrole in CH_2Cl_2 where the changes were recorded as a function of time.

ical studies were carried out in CH_2Cl_2 containing 0.1 M TBAP. The spectral changes obtained under the influence of an applied reducing potential in the thin layer cell are presented in Figure 3a and the data for the neutral and singly reduced corroles in the CH_2Cl_2 solvent containing 0.1 M TBAP are summarized in Table 2.

The neutral corroles **1–5** have a well-defined Soret band located between 396 and 420 nm and broad ill-defined Q-bands as seen in Figure 3a. Similar spectra have been reported for **0** under the same solution conditions [5,10]. Upon reduction of corroles **1–4**, the Soret band at decreases in intensity as a new red-shifted Soret band of higher intensity grows in at

Table 2. UV–vis spectral data of neutral and singly reduced copper corroles **0–5** in CH_2Cl_2 containing 0.1 M TBAP

	λ_{max}, nm ($\varepsilon \times 10^{-4}$ $M^{-1} \cdot cm^{-1}$)						
	Neutral			Singly reduced			
Cpd	Soret	Q-Band(s)		Soret	Q-Band(s)		Ref.
0	410 (7.2)	540 (0.4)	633 (0.2)	432 (9.0)	578 (1.3)	607 (1.8)	[10]
1	396 (6.8)	537 (0.8)	597 (0.5)	426 (8.5)	537 (1.8)	603 (1.6)	t.w
2	397 (9.2)		601 (0.6)	428 (11.9)	558 (2.4)	601 (1.6)	t.w
3	405 (7.3)	548 (0.9)	602 (0.6)	428 (11.6)	538 (1.9)	576 (2.0)	t.w
4	407 (8.1)	541 (0.6)	625 (0.4)	432 (8.3)	582 (1.2)	610 (1.5)	t.w
5	420 (3.8)	540 (0.5)	627 (0.4)	417 (3.4)	518 (1.3)	648 (1.0)	t.w

Structures of the compounds are given in Scheme 1.

t.w = this work.

426–432 nm along with two new Q-bands located at 537–582 nm and 576 to 610 nm. There are no near-IR bands characteristic of a corrole π-anion radical and the spectral changes in Figure 3a for **1–4** are consistent with (1) which specifies generation of $[CorCu^{II}]^-$, a compound which possesses an intact conjugated macrocycle (i.e. Cor^{3-}).

Copper corrole **5** exhibits slightly different behavior upon electroreduction. As seen in Figure 3a, the Soret band of **5** shifts by only 3 nm to higher energy wavelengths while the corresponding band for compounds **1–4** shifts by 23–31 nm to the red after reduction. Singly reduced **5** also has two broad and intense Q-bands at 518 and 648 nm, a spectral pattern quite different than is seen for singly reduced **0–4**. This difference between the UV–vis spectrum of singly reduced **5** and the singly reduced corroles **0–4** (as well as various other copper corroles [10,12,13]) might result from a change in the site of electron transfer, but the plot in Figure 2 does not lend credence to this explanation. Nonetheless, the final spectrum of singly reduced **5** possesses broad Q-bands in the visible region which appear similar to hyperporphyrin-type spectra reported for peripherally protonated free base tris(*p*-aminophenyl)corrole isomers [49], a phenomenon which might arise from a mesomeric effect of the *para*-nitro substituents which is known to enhance delocalization of the conjugated π electrons, thus stabilizing the single negative charge on the molecule *via* resonance [50–52].

The effect of cyanide anions (CN^-) on UV–vis spectra of the copper corroles was also examined and the time dependent spectral changes observed upon addition of an aliquot to give a 0.02 M $TBACN/CH_2Cl_2$ solution of **1–5** ($\sim 10^{-5}$ M) is shown in Figure 3b. In each case, the spectral changes seen upon the addition of CN^- are strikingly similar to what is seen for the same corroles under the application of an applied reducing potential (Figure 3a). Moreover, the final spectrum of each corrole after electrochemical or chemical conversion to its monoanionic form are identical to each other, thus providing clear evidence for the ability of cyanide anions to reduce the open-shell noninnocent $Cor^{\bullet}Cu^{II}$ to a $[CorCu^{II}]^-$ product according to (1) *via* anion induced electron transfer (AIET).

The time elapsed for conversion of the neutral copper corrole to its final chemically reduced form ranged from 23 s for corrole **3** to 1392 s for compound **1**. Moreover, a monotonic increase in the elapsed time needed to complete the AIET processes was observed with decrease in the first reduction potential of the compound (i.e. a more negative $E_{1/2}$ value). This trend is consistent with the thermodynamically driven electron transfer (ET) event from the HOMO of cyanide anion to the LUMO/SOMO-1 of the corrole "π-acid" complex [20–22] where the relative energies of the corrole LUMO/SOMO-1 are indirectly determined by the first reduction potential.

A simple diagram for this AIET process is given in Scheme 2, where the HOMO of the anion, in this case cyanide, lies at an energy level well above that of the open-shell copper corrole orbitals as detailed by
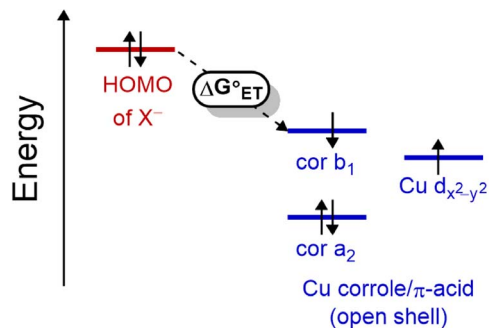
Scheme 2. Schematic energy diagram for the HOMOs of anions (X$^-$) and the LUMO/SOMO-1 of the open-shell copper corrole depicting thermal electron transfer (ET).
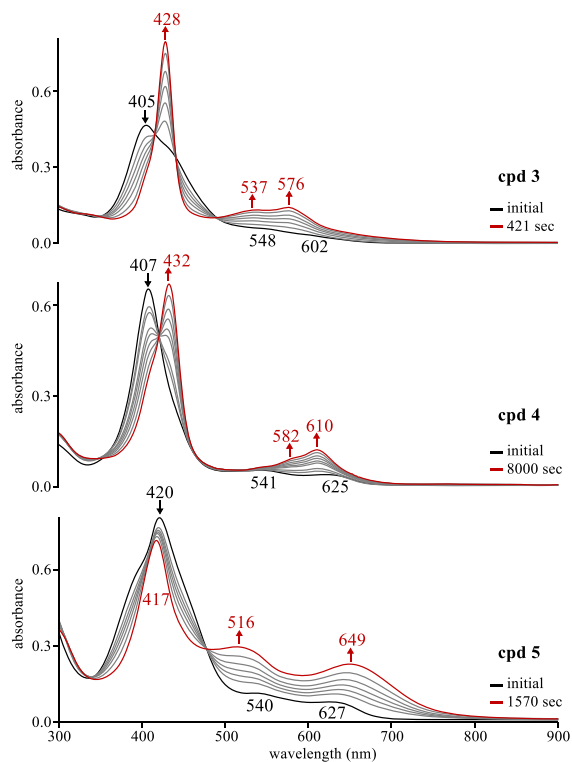

Figure 4. UV–vis spectral changes for compounds **3**–**5** upon addition of TBAF (0.05 M) to ~10^{-5} M corrole in CH$_2$Cl$_2$ where the changes are recorded as a function of time.

Figure 5. UV–vis spectral changes for reference corrole **0** (a) during an applied reducing potential (~10^{-4} M) in CH$_2$Cl$_2$ containing 0.1 M TBAP, (b) upon addition of TBACN (0.02 M) to ~10^{-5} M corrole in CH$_2$Cl$_2$ and (c) upon addition of TBAF (0.5 M) to ~10^{-5} M corrole in CH$_2$Cl$_2$ where the changes are recorded as a function of time.

Ghosh, Solomon and coworkers [6] as well as Nocera and coworkers [53].

Like in the case of cyanide anion, F$^-$ has also been shown to reduce π-acids [22] and was pre-
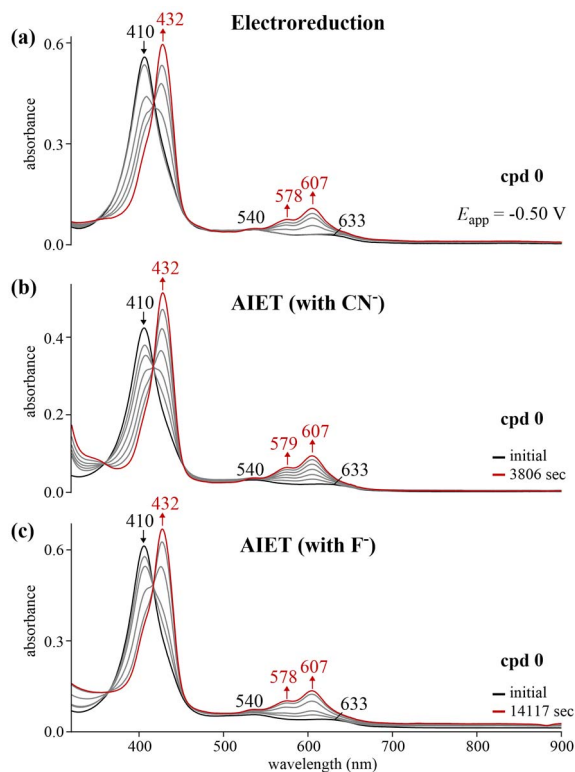
viously shown to reduce noninnocent cobalt corroles [19]. Thus, the ability of fluoride anions to reduce open-shell noninnocent copper corroles by the addition of TBAF to solution was also investigated in the current study. As seen in Figure 4, the addition of TBAF (0.05 M) to a CH$_2$Cl$_2$ solution of corroles **3**–**5** led to exactly the same pattern of spectral changes as seen for either electroreduction in a thin layer cell or chemical reduction via CN$^-$ (Figure 3). However, The time to complete reduction of these corroles by anion induced electron transfer was slower with F$^-$ than with CN$^-$ and this is shown by a comparison of the data for compounds **3**–**5** in Figure 3 with that which was observed in Figure 4 where the rates decreased by a fac-

tor of ~18 to 6.5 depending upon the substitution pattern.

Identical UV–visible were also observed for the electrochemically and chemically reduced parent compound **0** (Figure 5) but the time for reduction by anion induced electron transfer was slower for F⁻ than CN⁻ despite the ten-fold increase in the concentration of fluoride as compared to cyanide.

4. Conclusion

The mounting evidence for the ability of Lewis basic anions to reduce noninnocent corroles as described in the current study on copper corroles and also in our previous report for cobalt corroles [19] suggests that the occurrence of an anion induced electron transfer (AIET) event in aprotic media can serve as an additional probe for provisionally assigning the non-innocence or innocence of metallocorroles, particularly where there is a more cryptic noninnocent behavior as in the case of silver corrole derivatives [4,5].

Conflicts of interest

The authors declare no competing financial interest.

Acknowledgements

Supplementary data

¹H NMR of corroles **1–5** and ¹⁹F NMR of **3**. LRMS (ESI) spectra of corroles **1–5** and HRMS (ESI) spectra of **2** and **3**. ¹H NMR of (**Mes**)₂(**2,4-(NO₂)₂Ph**)**CorH₃** and LRMS and HRMS (ESI) for (**Mes**)₂(**2,4-(NO₂)₂Ph**)**CorH₃**.

Supporting information for this article is available on the journal's website under https://doi.org/10.5802/crchim.95 or from the author.

References

[1] J. F. B. Barata, M. G. P. M. S. Neves, M. A. F. Faustino, A. C. Tomé, J. A. S. Cavaleiro, *Chem. Rev.*, 2017, **117**, 3192-3253.
[2] S. Nardis, F. Mandoj, M. Stefanelli, R. Paolesse, *Coord. Chem. Rev.*, 2019, **388**, 360-405.
[3] Y. Fang, Z. Ou, K. M. Kadish, *Chem. Rev.*, 2017, **117**, 3377-3419.
[4] A. Ghosh, *Chem. Rev.*, 2017, **117**, 3798-3881.
[5] K. E. Thomas, H. Vazquez-Lima, Y. Fang, Y. Song, K. J. Gagnon, C. M. Beavers, K. M. Kadish, A. Ghosh, *Chem. Eur. J.*, 2015, **21**, 16839-16847.
[6] H. Lim, K. E. Thomas, B. Hedman, K. O. Hodgson, A. Ghosh, E. I. Solomon, *Inorg. Chem.*, 2019, **58**, 6722-6730.
[7] A. Ghosh, T. Wondimagegn, A. B. J. Parusel, *J. Am. Chem. Soc.*, 2000, **122**, 5100-5104.
[8] D. Shimizu, A. Osuka, *Chem. Sci.*, 2018, **9**, 1408-1423.
[9] K. Pierloot, H. Zhao, S. Vancoillie, *Inorg. Chem.*, 2010, **49**, 10316-10329.
[10] Z. Ou, J. Shao, H. Zhao, K. Ohkubo, I. H. Wasbotten, S. Fukuzumi, A. Ghosh, K. M. Kadish, *J. Porphyr. Phthalocyanines*, 2004, **08**, 1236-1247.
[11] L. Ye, Z. Ou, Y. Fang, Y. Song, B. Li, R. Liu, K. M. Kadish, *J. Porphyr. Phthalocyanines*, 2016, **20**, 753-765.
[12] F. Wu, J. Xu, H. Gao, C. Li, S. Xu, H. Uno, Y. Xu, Y. Zhao, Z. Shen, *Chem. Commun.*, 2021, **57**, 383-386.
[13] P. Yadav, M. Sankar, X. Ke, L. Cong, K. M. Kadish, *Dalton Trans.*, 2017, **46**, 10014-10022.
[14] A. Alemayehu, J. Conradie, A. Ghosh, *Eur. J. Inorg. Chem.*, 2011, **2011**, 1857-1864.
[15] S. Ganguly, A. Ghosh, *Acc. Chem. Res.*, 2019, **52**, 2003-2014.
[16] X. Jiang, M. L. Naitana, N. Desbois, V. Quesneau, S. Brandès, Y. Rousselin, W. Shan, W. R. Osterloh, V. Blondeau-Patissier, C. P. Gros, K. M. Kadish, *Inorg. Chem.*, 2018, **57**, 1226-1241.
[17] X. Jiang, W. Shan, N. Desbois, V. Quesneau, S. Brandès, E. V. Caemelbecke, W. R. Osterloh, V. Blondeau-Patissier, C. P. Gros, K. M. Kadish, *New J. Chem.*, 2018, **42**, 8220-8229.
[18] W. R. Osterloh, N. Desbois, V. Quesneau, S. Brandes, P. Fleurat-Lessard, Y. Fang, V. Blondeau-Patissier, R. Paolesse, C. P. Gros, K. M. Kadish, *Inorg. Chem.*, 2020, **59**, 8562-8579.
[19] W. R. Osterloh, V. Quesneau, N. Desbois, S. Brandès, W. Shan, V. Blondeau-Patissier, R. Paolesse, C. P. Gros, K. M. Kadish, *Inorg. Chem.*, 2020, **59**, 595-611.
[20] S. Guha, S. Saha, *J. Am. Chem. Soc.*, 2010, **132**, 17674-17677.
[21] G. Aragay, A. Frontera, V. Lloveras, J. Vidal-Gancedo, P. Ballester, *J. Am. Chem. Soc.*, 2013, **135**, 2620-2627.
[22] S. Saha, *Acc. Chem. Res.*, 2018, **51**, 2225-2236.
[23] I. H. Wasbotten, T. Wondimagegn, A. Ghosh, *J. Am. Chem. Soc.*, 2002, **124**, 8104-8116.
[24] D. T. Gryko, K. Jadach, *J. Org. Chem.*, 2001, **66**, 4267-4275.
[25] T. H. Ngo, W. Van Rossom, W. Dehaen, W. Maes, *Org. Biomol. Chem.*, 2009, **7**, 439-443.
[26] S. Kappler-Gratias, L. Bucher, N. Desbois, Y. Rousselin, K. Bystricky, C. P. Gros, F. Gallardo, *RSC Med. Chem.*, 2020, **11**, 783-801.

[27] C. Gros, F. Gallardo, N. Desbois, "Preparation of Corrole Compounds and Methods of Use Thereof for Treating Poxvirus Infection", 2019, *PCT Int. Appl.* WO2019105940A1.

[28] C. Gros, F. Gallardo, N. Desbois, "Preparation of Corrole Compounds and Methods of Use Thereof for Treating Human Cytomegalovirus Infections", 2019, *PCT Int. Appl.* WO2019105928A1.

[29] M. Li, Y. Niu, W. Zhu, J. Mack, G. Fomo, T. Nyokong, X. Liang, *Dyes Pigments*, 2017, **137**, 523-531.

[30] R. Paolesse, S. Nardis, F. Sagone, R. G. Khoury, *J. Org. Chem.*, 2001, **66**, 550-556.

[31] D. Bhattacharya, P. Singh, S. Sarkar, *Inorg. Chim. Acta*, 2010, **363**, 4313-4318.

[32] H. Lei, H. Fang, Y. Han, W. Lai, X. Fu, R. Cao, *ACS Catal.*, 2015, **5**, 5145-5153.

[33] S. Ganguly, J. Conradie, J. Bendix, K. J. Gagnon, L. J. McCormick, A. Ghosh, *J. Phys. Chem. A*, 2017, **121**, 9589-9598.

[34] V. Quesneau, W. Shan, N. Desbois, S. Brandès, Y. Rousselin, M. Vanotti, V. Blondeau-Patissier, M. Naitana, P. Fleurat-Lessard, E. Van Caemelbecke, K. M. Kadish, C. P. Gros, *Eur. J. Inorg. Chem.*, 2018, **2018**, 4265-4277.

[35] T. Kitagawa, T. P. Layloff, R. N. Adams, *Anal. Chem.*, 1963, **35**, 1086-1087.

[36] K. M. Kadish, E. Wenbo, P. J. Sintic, Z. Ou, J. Shao, K. Ohkubo, S. Fukuzumi, L. J. Govenlock, J. A. McDonald, A. C. Try, Z.-L. Cai, J. R. Reimers, M. J. Crossley, *J. Phys. Chem. B*, 2007, **111**, 8762-8774.

[37] D. H. Geske, J. L. Ragle, M. A. Bambenek, A. L. Balch, *J. Am. Chem. Soc.*, 1964, **86**, 987-1002.

[38] I. M. Sosonkin, G. N. Strogov, T. K. Ponomareva, A. N. Domarev, A. A. Glushkova, G. N. Freidlin, *Chem. Heterocycl. Comp.*, 1981, **17**, 137-140.

[39] S. Nardis, M. Stefanelli, P. Mohite, G. Pomarico, L. Tortora, M. Manowong, P. Chen, K. M. Kadish, F. R. Fronczek, G. T. McCandless, K. M. Smith, R. Paolesse, *Inorg. Chem.*, 2012, **51**, 3910-3920.

[40] Y. Fang, X. Jiang, Z. Ou, C. Michelin, N. Desbois, C. P. Gros, K. M. Kadish, *J. Porphyr. Phthalocyanines*, 2014, **18**, 832-841.

[41] A. Ghosh, I. Halvorsen, H. J. Nilsen, E. Steene, T. Wondimagegn, R. Lie, E. van Caemelbecke, N. Guo, Z. Ou, K. M. Kadish, *J. Phys. Chem. B*, 2001, **105**, 8120-8124.

[42] M. Mohammad, A. Y. Khan, M. Afzal, A. Nisa, R. Ahmed, *Aust. J. Chem.*, 1974, **27**, 2495-2498.

[43] K. M. Kadish, V. A. Adamian, E. Van Caemelbecke, E. Gueletii, S. Will, C. Erben, E. Vogel, *J. Am. Chem. Soc.*, 1998, **120**, 11986-11993.

[44] K. M. Kadish, M. M. Morrison, *J. Am. Chem. Soc.*, 1976, **98**, 3326-3328.

[45] K. M. Kadish, M. M. Morrison, *Inorg. Chem.*, 1976, **15**, 980-982.

[46] K. M. Kadish, M. M. Morrison, *Bioinorg. Chem.*, 1977, **7**, 107-115.

[47] K. M. Kadish, E. Van Caemelbecke, G. Royal, "Electrochemistry of metalloporphyrins in nonaqueous media", in *The Porphyrin Handbook* (K. M. Kadish, K. M. Smith, R. Guilard, eds.), vol. 8, Academic Press, Burlington, MA, 2000, 1-97.

[48] A. Ghosh, E. Steene, *J. Inorg. Biochem.*, 2002, **91**, 423-436.

[49] I. K. Thomassen, A. Ghosh, *ACS Omega*, 2020, **5**, 9023-9030.

[50] C. Hansch, A. Leo, R. W. Taft, *Chem. Rev.*, 1991, **91**, 165-195.

[51] O. Exner, T. M. Krygowski, *Chem. Soc. Rev.*, 1996, **25**, 71-75.

[52] E. V. A. D. A. Dougherty, "Experiments related to thermodynamics and kinetics", in *Modern Physical Organic Chemistry*, University Science Books, Mill Valley, California, 2006, 421-488.

[53] C. M. Lemon, M. Huynh, A. G. Maher, B. L. Anderson, E. D. Bloch, D. C. Powers, D. G. Nocera, *Angew. Chem. Int. Ed.*, 2016, **55**, 2176-2180.